Pharmacological Research 178 (2022) 106137

Contents lists available at ScienceDirect

Pharmacological Research

journal homepage: www.elsevier.com/locate/yphrs

ABCB1 limits brain exposure of the KRAS^{G12C} inhibitor sotorasib, whereas ABCB1, CYP3A, and possibly OATP1a/1b restrict its oral availability

Nancy H.C. Loos [a], Irene A. Retmana [a,b], Wenlong Li [a], Margarida L.F. Martins [a], Maria C. Lebre [a], Rolf W. Sparidans [b], Jos H. Beijnen [a,c,d], Alfred H. Schinkel [a,*]

[a] The Netherlands Cancer Institute, Division of Pharmacology, Amsterdam, The Netherlands
[b] Utrecht University, Faculty of Science, Department of Pharmaceutical Sciences, Division of Pharmacology, Utrecht, The Netherlands
[c] Utrecht University, Faculty of Science, Department of Pharmaceutical Sciences, Division of Pharmacoepidemiology and Clinical Pharmacology, Utrecht, The Netherlands
[d] The Netherlands Cancer Institute, Division of Pharmacy and Pharmacology, Amsterdam, The Netherlands

ARTICLE INFO

Keywords:
Sotorasib
KRAS^{G12C} inhibitor
ABCB1/P-glycoprotein
ABCG2/Breast cancer resistance protein
Cytochrome P450 3A
Pharmacokinetics

Chemical compounds studied in this article:
Sotorasib (PubChem CID 137278711)
Elacridar HCl (PubChem CID: 170320)
Zosuquidar (PubChem CID: 153997)
Ko143 (PubChem CID 10322450)

ABSTRACT

Sotorasib (Lumakras™) is the first FDA-approved KRAS^{G12C} inhibitor for treatment of patients with non-small cell lung cancer (NSCLC) carrying this mutation. Using genetically modified mouse models, we studied the influence of the efflux transporters ABCB1 and ABCG2, the OATP1a/1b uptake transporters, and the CYP3A drug-metabolizing enzyme complex on the plasma pharmacokinetics and tissue distribution of oral sotorasib. *In vitro*, sotorasib was a potent substrate for human ABCB1 and a modest substrate for mouse Abcg2, but not for human ABCG2. *In vivo*, the brain-to-plasma ratio of sotorasib (40 mg/kg) was highly increased in *Abcb1a/1b*$^{-/-}$ (5.9-fold) and *Abcb1a/1b;Abcg2*$^{-/-}$ (7.6-fold) compared to wild-type mice, but not in single *Abcg2*$^{-/-}$ mice. Upon coadministering elacridar, an ABCB1/ABCG2 inhibitor, sotorasib brain accumulation increased 7.5-fold, approaching the levels observed in Abcb1a/1b-deficient mice. No acute CNS toxicity emerged upon boosting of the sotorasib exposure. In Oatp1a/1b-deficient mice, we observed a 2-fold reduction in liver disposition compared to wild-type mice, although these uptake transporters had no noticeable impact on sotorasib plasma exposure. However, plasma exposure was limited by mouse Cyp3a and human CYP3A4, as the $AUC_{0-4\ h}$ in *Cyp3a*$^{-/-}$ mice was increased by 2.5-fold compared to wild-type mice, and subsequently strongly decreased (by 3.9-fold) in Cyp3aXAV mice transgenically overexpressing human CYP3A4 in liver and intestine. Collectively, the oral availability of sotorasib was markedly limited by CYP3A and possibly also by ABCB1 and OATP1a/b, whereas its brain accumulation was strongly restricted by ABCB1. The obtained results may help to further optimize the safety and efficacy of sotorasib in clinical use.

1. Introduction

Mutations in the Kirsten rat sarcoma viral oncogene homolog (KRAS) are involved in human tumor cell growth and survival [1–3]. The KRAS^{G12C}-mutant occurs in approximately 13% of lung adenocarcinoma, 3% of colorectal cancers and 2% of other solid tumors, and patients suffering from cancers with this KRAS mutation have been associated with a poor prognosis [3–6]. Although mutant KRAS was long seen as an "undruggable" target, recently several KRAS^{G12C} inhibitors have entered clinical trials, of which sotorasib (AMG-510) was the first (Suppl. Fig. 1) [1,7,8]. Sotorasib (Lumakras™) is a selective KRAS^{G12C} inhibitor recently approved (May 2021) by the Food and Drug Administration (FDA) for patients with locally advanced or metastatic KRAS^{G12C}-mutated non-small cell lung cancer (NSCLC) previously

Abbreviations: ABC, ATP-binding cassette; ANOVA, analysis of variance; AUC, area under the plasma concentration-time curve; BBB, blood-brain barrier; BCRP/ABCG2, Breast Cancer Resistance Protein; BSA, bovine serum albumin; C_{max}, peak plasma concentration; CYP, cytochrome P450; DMEM, Dulbecco's modified essential medium; DMSO, dimethyl sulfoxide; DPBS, Dulbecco's phosphate-buffered saline; FBS, fetal bovine serum; FDA, Food and Drug Administration; FVB, Friend Virus B; GDP, guanosine diphosphate; GTP, guanosine triphosphate; KRAS, Kirsten rat sarcoma virus; LC-MS/MS, liquid chromatography-tandem mass spectrometry; MAPK, RAF-MEK-ERK; MDCK-II, Madin-Darby Canine Kidney II; NSCLC, non-small cell lung cancer; OATP/SLCO, organic anion-transporting polypeptides; p-ERK, phosphorylation of ERK1/2; P-glycoprotein, P-gp/ABCB1/MDR1; SD, standard deviation; TEER, transepithelial electrical resistance; T_{max}, time to reach peak plasma concentration; Zos, zosuquidar.

* Correspondence to: Division of Pharmacology, The Netherlands Cancer Institute, Plesmanlaan 121, 1066 CX Amsterdam, The Netherlands.
E-mail address: a.schinkel@nki.nl (A.H. Schinkel).

https://doi.org/10.1016/j.phrs.2022.106137
Received 8 December 2021; Received in revised form 2 February 2022; Accepted 17 February 2022
Available online 19 February 2022

treated with at least one systemic therapy [9]. The approved dose for sotorasib tablets is 960 mg once daily [9]. In mice with xenografts of human $KRAS^{G12C}$ tumors, sotorasib showed tumor volume regression in every dosing cohort, although the durability was less in mice with a lower dosing level (10 mg/kg *vs.* 100 mg/kg) [8]. However, many pharmacokinetic data on sotorasib are still lacking, especially the tissue distribution profile and brain penetration of sotorasib.

Insights into the determinants of the pharmacokinetics of drugs can provide clinicians information on drug-drug interactions and drug efficacy and safety [10,11]. The ATP-binding cassette (ABC) transporter superfamily is a family of efflux transporters, among which P-glycoprotein (P-gp/MDR1/ABCB1) and Breast Cancer Resistance Protein (BCRP/ABCG2) are important members with broad substrate specificities [12]. These efflux transporters reside in the luminal (apical) membrane of polarized cells in several organs, mainly the liver, small intestine and kidney [13]. ABCB1 and ABCG2 can limit intestinal absorption and contribute to direct hepatic, intestinal or renal excretion of substrate drugs [11,13,14]. Furthermore, these transporters can play an important role in restricting the brain penetration of substrate drugs, because they are expressed at the luminal side of the blood-brain-barrier (BBB) [15–17]. This limited brain exposure may affect the efficacy of those drugs against brain (micro-)metastases [18,19]. Significant brain penetration of sotorasib could be important, because the incidence of brain metastasis in $KRAS^{G12C}$-mutated NSCLC is approximately 50% [20].

The uptake transporter superfamily of organic anion-transporting polypeptides (OATPs; SLCO) facilitates the cellular influx of several drugs and compounds. The subfamily members OATP1B1, OATP1B3, and OATP2B1 are expressed in the sinusoidal membrane of the hepatocytes and mediate liver uptake of their substrate compounds, but the significance of OATP1A2 function and expression in the human intestine is doubtful [21,22].

Drug-metabolizing enzymes can also impact the pharmacokinetics of substrate drugs. Cytochrome P450 (CYP) 3A4, a prominent member of the CYP superfamily, is abundant in human liver and small intestine [23,24]. CYP3A4 can restrict the oral bioavailability and overall systemic exposure of its substrate drugs, which are structurally highly diverse [24]. Moreover, CYP3A4 is susceptible to wide inter- and intra-individual variation in its activity due to genetic polymorphisms as well as inhibition or induction by other drugs and compounds, leading to variable drug exposure in patients [23–25]. As mentioned in the FDA approval documentation, sotorasib is a CYP3A substrate [9], however, it was still unknown to what extent. Therefore, it is important to establish to what extent sotorasib is a CYP3A substrate *in vivo* and whether this might result in substantial pharmacokinetic changes.

The FDA registration information provides limited information about the possible transport of sotorasib by ABC or OATP transporters [9]: Coadministration with P-gp/ABCB1 substrates should be avoided, indicating that sotorasib is a substrate and inhibitor for ABCB1. In addition, sotorasib might inhibit BCRP/ABCG2 [9]. However, the extent of this transport is unclear and the impact of these transporters on the tissue distribution of sotorasib is not elucidated yet. Information regarding the OATP influx transporters is also limited. The drug-drug interaction studies showed no meaningful differences after administration of a single dose of rifampin, an OATP1B1/1B3 inhibitor, suggesting sotorasib is not a substantial substrate of these transporters. Finally, avoidance of coadministering CYP3A4-sensitive substrates with a narrow therapeutic window with sotorasib is recommended, indicating inhibition of CYP3A4 by sotorasib. CYP3A also mediates the oxidative metabolism of sotorasib itself and therefore repeated doses of strong CYP3A inducers should be used with caution [9].

The aim of this study was to gain more insight into the influence of ABCB1 and ABCG2 on sotorasib transport *in vitro* and to establish to what extent these efflux transporters, OATP1A/1B uptake transporters, and the drug-metabolizing enzyme CYP3A can affect the oral availability and tissue distribution of sotorasib. We used Abcb1, Abcg2, and Oatp1a/1b knockout mouse strains to investigate this impact. Using Cyp3a knockout and CYP3A4-humanized transgenic mouse models we further evaluated the impact of this enzyme complex on sotorasib pharmacokinetics.

2. Materials and methods

2.1. Chemicals

Sotorasib (AMG-510) was purchased from MedChem Express (Monmouth Junction, NJ). Zosuquidar (Zos) was obtained from Sequoia Research Products (Pangbourne, United Kingdom) and Ko143 from Tocris Bioscience (Abingdon, United Kingdom). Elacridar HCl was obtained from Biosynth (Bratislava, Slovakia). Bovine Serum Albumin (BSA) Fraction V was supplied by Roche Diagnostics (Mannheim, Germany). Glucose water (5%, w/v) was obtained from B. Braun Medical Supplies (Melsungen, Germany). Isoflurane was purchased from Virbac Nederland (Barneveld, The Netherlands), heparin (5000 IU mL^{-1}) was obtained from Leo Pharma (Breda, The Netherlands). Other chemicals and reagents used in the assay of sotorasib were described before [26]. All other reagents and chemicals were supplied by Sigma-Aldrich (Steinheim, Germany).

For cell culture, Dulbecco's Modified Essential Medium (DMEM) glutamax, penicillin-streptomycin 10,000 U/L, and Dulbecco's Phosphate-Buffered saline (DPBS) were purchased from Life Technologies (Bleiswijk, The Netherlands). Fetal Bovine Serum (FBS) was supplied by Serana (Pessin, Germany).

2.2. Cell lines

Parental Madin–Darby Canine Kidney cells (MDCK-II, European Collection of Cell Cultures, ECACC 00062107) and subclones that are stably transduced with human (h) ABCB1, hABCG2, or mouse (m) Abcg2 cDNA were grown at 37 °C in 5% CO_2 [27–29]. All cell lines were mycoplasma free. The cell lines were cultured in supplemented culture medium (DMEM with 10% (v/v) FBS and 1% (v/v) of penicillin-streptomycin stock). For the transport experiments, cells were cultured for at least 2 weeks, resulting in a passage number between 8 and 13.

2.3. Drug transporter assay

In vitro transepithelial drug transport assays were performed using 12-well plates with microporous polycarbonate membrane filter inserts (3.0-μm pore size, 12-mm diameter, Transwell 3402, Corning; Amsterdam, The Netherlands). The parental MDCK-II cells and the transduced cell lines were seeded at a density of 2.5×10^5 cells per well and the cells were grown for 3 days to allow the formation of an intact monolayer. On day 1 and 2 after seeding of the cells, the culture medium was replaced. Transepithelial electrical resistance (TEER) levels were measured to confirm the integrity of the monolayer membranes before and after the transport experiment, where all levels were within the reference values ($\geq$ 70 Ω cm^2 for the parental and hABCG2-overexpressing, $\geq$ 200 Ω cm^2 for the hABCB1-overexpressing, and $\geq$ 140 Ω cm^2 for the mAbcg2-overexpressing cell line).

Sotorasib was dissolved in dimethyl sulfoxide (DMSO) at a concentration of 4 mM, and further diluted 1000-fold with DMEM medium containing 10% (v/v) FBS resulting in a 4 μM working solution. The inhibitors zosuquidar (ABCB1 inhibitor) and Ko143 (ABCG2/Abcg2 inhibitor) were dissolved in DMSO at a concentration of 2 mM, and further diluted 1000-fold with DMEM medium containing 10% (v/v) FBS resulting in 2 μM working solutions. First, cells were preincubated with medium or medium with the inhibitor(s) in both compartments for 1 h. Subsequently, the transport phase was initiated (t = 0) by replacement of the medium in the donor compartment (either basolateral or apical) by fresh medium containing 10% FBS, 4 μM sotorasib and, where

appropriate, 2 μM inhibitor(s), respectively. The cells were kept at 37 °C, pH 7.4, in a 5% (v/v) CO_2 environment. Sample collection (50 μL) from the acceptor compartment was performed at 1, 2, 4, and 8 h after the start. Before bioanalytical pretreatment and measurement, the samples were stored at − 30 °C. To evaluate active transport of sotorasib, the transport ratio r was calculated by dividing the degree of transport in the apical direction by the degree of transport in the basolateral direction after 8 h.

2.4. Animals

Mice were housed and handled according to institutional guidelines complying with Dutch and EU legislation. All experimental animal protocols (under national permit number AVD301002016595) were approved by the institutional board for care and use of laboratory animals. For these sotorasib experiments female wild-type, *Abcb1a/1b*$^{-/-}$, *Abcg2*$^{-/-}$, *Abcb1a/1b;Abcg2*$^{-/-}$, *Oatp1a/b*$^{-/-}$, *Cyp3a*$^{-/-}$, and Cyp3aXAV (overexpression of human CYP3A in liver and intestine of *Cyp3a*$^{-/-}$) mice were used. Sotorasib is clinically applied in both males and females. As there are no indications for pronounced gender differences for the studied drug transporters and metabolizing enzymes in mice, we limited our analyses to female mice in order to optimize (minimize) the usage of all generated mice, as is legally required. Male mice were used for other drug studies. All animals have a > 99% FVB genetic background, and they were used between 9 and 16 weeks of age. Mice were kept in a specific pathogen-free, temperature-controlled environment with a 12-hour light and 12-hour dark cycle, and they received a standard diet (Transbreed, SDS Diets, Technilab-BMI, Someren, The Netherlands) and acidified water *ad libitum*. Animal welfare assessments were performed before, during, and after the experiments.

2.5. Drug solutions

For oral administration, sotorasib was dissolved in DMSO at a concentration of 50 mg/mL, and further diluted with polysorbate 80/ethanol (1:1, v/v), and 5% (w/v) glucose in water to yield a concentration of 2 mg/mL or 4 mg/mL in the dosing solution, depending on the experiment. Final concentrations of DMSO, polysorbate 80, ethanol, and glucose in the dosing solution of 2 mg/mL were 4%, 3%, 3% (v/v), and 4.5% (w/v); in the dosing solution of 4 mg/mL 8%, 6%, 6% (v/v), and 4% (w/v), respectively. Elacridar hydrochloride was dissolved in DMSO at 53 mg/mL to obtain 50 mg elacridar base per mL. The stock solution of elacridar was further diluted 10-fold with a mixture of polysorbate 80, ethanol and water [20:13:67 (v/v/v)], to reach a concentration of 5 mg/mL in the oral dosing solution. The vehicle dosing solution contained 10% DMSO, 15% polysorbate 80, 15% ethanol, and 60% water (v/v). All dosing solutions were prepared freshly on the day of the experiment.

2.6. Plasma pharmacokinetics and tissue distribution of sotorasib in mice

Before all oral administrations of sotorasib, mice were fasted for 2–3 h to minimize variation in oral drug absorption.

2.6.1. Pilot experiment in *Abcb1a/1b;Abcg2*$^{-/-}$, and *Oatp1a/b*$^{-/-}$ mice

Sotorasib (20 mg/kg of body weight; 2 mg/mL dosing solution) was administered by gavage into the stomach, with a blunt-ended needle, to wild-type, *Abcb1a/1b;Abcg2*$^{-/-}$, and *Oatp1a/b*$^{-/-}$ (1-hour experiment). Tail vein blood (~50 μL per sample) sampling was performed at respectively 5, 10, 15, 30, and 60 min after administration of sotorasib, using heparinized microvettes.

2.6.2. Impact of single Abcb1a/1b and Abcg2 transporters on pharmacokinetics and tissue distribution of sotorasib

In this follow-up experiment, wild-type, *Abcb1a/1b*$^{-/-}$, *Abcg2*$^{-/-}$, and *Abcb1a/1b;Abcg2*$^{-/-}$ mice were used in a 30-minutes experiment. Tail vein blood sampling (~50 μL per sample) was performed at 5, 10, and 15 min, after oral administration of sotorasib (40 mg/kg of body weight; 4 mg/mL dosing solution).

2.6.3. Impact of Oatp1a/1b transporters on pharmacokinetics and tissue distribution of sotorasib

In this follow-up experiment, *Oatp1a/b*$^{-/-}$ mice received sotorasib at a dose of 40 mg/kg of body weight (4 mg/mL dosing solution) by oral gavage in a 15-minutes experiment. Blood (~50 μL per sample) was collected from the tail vein at 5, and 10 min after the sotorasib administration.

2.6.4. Impact of CYP3A enzyme on pharmacokinetics and tissue distribution of sotorasib

Sotorasib (20 mg/kg of body weight; 2 mg/mL dosing solution) was administered orally by gavage to wild-type, *Cyp3a*$^{-/-}$, and Cyp3aXAV mice in a 4-hour experiment. Tail vein blood (~50 μL per sample) sampling was performed at respectively 0.125, 0.25, 0.5, 1, and 2 h after administration of sotorasib, using heparinized microvettes.

2.6.5. Termination of animal experiments

At the end of each experiment, mice were anesthetized using an isoflurane evaporator with 3% isoflurane with 0.8 L/min air and 0.3 L/min oxygen. Blood was then collected by cardiac puncture, using Eppendorf tubes containing heparin as an anticoagulant. Subsequently, the anesthetized mice were sacrificed by cervical dislocation, and brain, liver, spleen, kidney, small intestine, and lungs were collected. The small intestinal content (SIC) was also collected by separating this from small intestinal tissue, which was rinsed with saline to remove possible residual feces. Plasma was isolated from the blood by centrifugation at 9000×*g* for 6 min at 4 °C, and the plasma fraction was collected and stored at − 30 °C until analysis. Brain, liver, spleen, kidney, small intestinal tissue, SIC, and lung were homogenized in a FastPrep-24TM 5 G homogenizer (M.P. Biomedicals, Santa Ana, CA) for 1 min with 1, 3, 1, 2, 3, 2, and 1 mL of 2% (w/v) BSA, respectively. All samples were stored at − 30 °C until analysis.

2.7. Sotorasib boosting study with orally administered elacridar

Prior to fasting, elacridar (50 mg/kg of body weight; 5 mg/mL dosing solution) or vehicle solution was orally administered to wild-type and *Abcb1a/1b;Abcg2*$^{-/-}$ mice. Before oral administration of sotorasib (40 mg/kg of body weight; 4 mg/mL dosing solution), mice were fasted for at least 3 h, as described above. Subsequently, tail vein blood collection was performed at 5, 10, and 15 min. The experiment was terminated as described above by performing cardiac puncture at 1 h after administration of sotorasib, and the same organs were collected. In this experiment, the small intestine tissue was collected together with the small intestinal content. All samples were processed and stored as described above.

2.8. Bioanalytical analysis

A recently developed liquid chromatography-tandem mass spectrometry (LC-MS/MS) method [26] was used to measure the concentrations of sotorasib in DMEM cell culture medium, plasma samples, and tissue homogenates. This method was partially validated for plasma and tissue samples, but not for DMEM medium samples. The LC-MS/MS settings are similar for all the measured samples, however the sample preparation and calibration range of the assay for the DMEM samples were slightly different, as described in the Supplemental data.

2.9. Pharmacokinetic calculations and statistical analysis

Pharmacokinetic parameters were calculated using non-compartmental methods using the software package of PK solutions 2.0.2 (SUMMIT, Research Service, Montrose, CO). The area under the

curve (AUC) of sotorasib was calculated using the linear trapezoidal rule without extrapolating to infinity. The peak plasma concentration (C_{max}) and time of peak plasma concentration (T_{max}) were assessed from the raw data from each individual mouse. GraphPad Prism 9 (GraphPad Software Inc., La Jolla, CA) was used for graphs and statistical analysis. The Grubbs' test was used to identify possible outliers. The two-sided unpaired Student t-test was used for the comparison of two groups, whereas one-way analysis of variance (ANOVA) was used for the comparison of multiple groups. Sidak's *post hoc* correction was applied to account for multiple comparisons. Differences were considered statistically significant, when $P < 0.05$. All data are presented as geometric mean ± SD.

3. Results

3.1. In vitro transport of sotorasib in ABC transporter-overexpressing MDCK-II cells

An *in vitro* transepithelial drug transport assay was performed to assess whether and to what extent sotorasib is a substrate transported by ABCB1 and ABCG2 using a parental Madin-Darby Canine Kidney (MDCK-II) cell line and its transduced subclones overexpressing hABCB1, hABCG2, and mAbcg2. In the parental MDCK-II cell line, sotorasib (4 μM) was actively transported to the apical side (transport ratio r = 10.7, Fig. 1A), presumably by the low-level endogenous canine Abcb1, as its transport could be fully inhibited by the ABCB1 inhibitor zosuquidar (2 μM) (r = 1.19, Fig. 1B). In the MDCK-II-hABCB1 cells, sotorasib was highly effectively transported to the apical side of the cells (r = 30.0, Fig. 1C), and this transport was inhibited by adding zosuquidar (r = 1.25, Fig. 1D). In the experiments with MDCK-II-hABCG2 and MDCK-II-mAbcg2 cells, zosuquidar was added to the medium to avoid any transport contribution of canine Abcb1. There was no detectable apically directed transport of sotorasib in the hABCG2-overexpressing cell line, as sotorasib was similarly translocated in both directions independent of absence or presence of the ABCG2 inhibitor Ko143 (r = 1.26 and r = 1.21, Fig. 1E and F). In the MDCK-II-mAbcg2 cells, slight apically directed transport of sotorasib was observed (r = 2.49, Fig. 1G), which could be inhibited by Ko143 (r = 1.17, Fig. 1H). Therefore, sotorasib appears to be efficiently transported by hABCB1 and slightly by mAbcg2, whereas it is not noticeably transported by hABCG2 *in vitro*.

3.2. Brain exposure of sotorasib is highly restricted by ABC transporters

As the *in vitro* data showed significant transport of sotorasib by hABCB1 and mAbcg2, the potential influence of these transporters on the pharmacokinetics of sotorasib was assessed in an *in vivo* pilot experiment using wild-type and *Abcb1a/1b;Abcg2*$^{-/-}$ mice. Sotorasib was orally administered at a dose of 20 mg/kg of body weight. The plasma $AUC_{0–60\ min}$ and C_{max} were not significantly different between wild-type and *Abcb1a/1b;Abcg2*$^{-/-}$ mice (Fig. 2A and B, Suppl. Table 1, $P > 0.05$), suggesting there is no influence of ABC transporters on plasma exposure to sotorasib at this dose. Furthermore, the role of ABCB1 and ABCG2 in tissue distribution of sotorasib was investigated. We observed a strong increase (15-fold) in the brain-to-plasma ratio of *Abcb1a/1b;Abcg2*$^{-/-}$ compared to wild-type mice (Fig. 2C and D, Suppl. Table 1, $P < 0.0001$), indicating that the brain exposure of sotorasib is strongly restricted by ABC transporters. The wild-type brain concentration was only 2.0% of the plasma concentration, *vs.* 30% in *Abcb1a/1b;Abcg2*$^{-/-}$ mice.

Furthermore, in SIC, the percentage of sotorasib recovered from the administered dose was dramatically decreased in *Abcb1a/1b;Abcg2*$^{-/-}$ mice at 1 h (11.7-fold, from 6.56% to 0.56%, $P < 0.0001$, Fig. 2G, Suppl. Table 1). The small intestine tissue concentrations seemed to reflect the SIC concentrations, with *Abcb1a/1b;Abcg2*$^{-/-}$ mice showing reduced small intestine tissue-to-plasma ratios (Fig. 2E–H). The results for SIC could be explained by hepatobiliary excretion of sotorasib or by active transport of the drug from the intestinal epithelium back into the intestinal lumen by these ABC transporters, or possibly a combination of these processes. The sotorasib disposition in the other analyzed tissues was not meaningfully affected in *Abcb1a/1b;Abcg2*$^{-/-}$ compared to wild-type mice (Suppl. Fig. 2).

To investigate the pharmacokinetic influence of the single ABCB1 and ABCG2 transporters, a follow-up experiment was performed, including single *Abcb1a/1b*$^{-/-}$ and *Abcg2*$^{-/-}$ mice. This experiment was terminated at 30 min to assess tissue distribution at a relatively high systemic drug concentration. We further increased the sotorasib dose to 40 mg/kg, as the 20 mg/kg used in the pilot resulted in pharmacokinetic parameters (AUC and C_{max}) that were two-fold lower than in humans, respectively a plasma $AUC_{0–24\ h}$ of 65.3 μg/mL*h and a C_{max} of 7.50 μg/mL [4]. Like in the pilot, no statistically significant differences were found in $AUC_{0–30\ min}$ and C_{max} between the four strains (Fig. 3A and B, Suppl. Table 1, $P > 0.05$). The brain-to-plasma ratio of sotorasib was again strongly increased in *Abcb1a/1b;Abcg2*$^{-/-}$ mice, but slightly less in single *Abcb1*$^{-/-}$ mice, by respectively 7.6- and 5.9-fold (Fig. 3C, Suppl. Table 1, $P < 0.0001$), compared to wild-type. No significant increase was found in the brain-to-plasma ratio in single *Abcg2*$^{-/-}$ mice. These results indicate that especially Abcb1 is responsible for limiting the brain exposure of sotorasib, whereas Abcg2 may perhaps additionally limit the brain concentration. In both pilot and follow-up experiments, the brain-to-plasma ratios in wild-type mice were very low (1.96% and 2.59%, respectively, compared to 30.0% and 19.8% in *Abcb1a/1b;Abcg2*$^{-/-}$ mice), indicating poor intrinsic brain penetration of sotorasib.

Moreover, consistent with the pilot, the percentage of sotorasib dose recovered in SIC was, albeit not significantly, decreased in *Abcb1a/1b*$^{-/-}$ and *Abcb1a/1b;Abcg2*$^{-/-}$ (2.0- and 2.7-fold, Fig. 3G, Suppl. Table 1), compared to wild-type mice. No marked shift was seen in *Abcg2*$^{-/-}$ mice. However, the small intestine-to-plasma ratios in *Abcb1a/1b*$^{-/-}$ and *Abcb1a/1b;Abcg2*$^{-/-}$ were significantly reduced (2.4- and 2.6-fold, respectively) compared to wild-type mice (Fig. 3F), suggesting the involvement of Abcb1a/1b in the intestinal disposition of sotorasib. The distribution of sotorasib to the other measured tissues was not meaningfully affected by absence of these ABC transporters (Suppl. Figs. 2 and 3), except perhaps for the lung-to-plasma ratios, which were significantly increased for *Abcb1a/1b*$^{-/-}$ and *Abcb1a/1b;Abcg2*$^{-/-}$ compared to wild-type mice, respectively ($P < 0.01$ and $P < 0.05$, Suppl. Fig. 3H).

In summary, the plasma exposure of sotorasib was not noticeably restricted by Abcb1a/b or Abcg2. The brain exposure of sotorasib was especially limited by Abcb1a/b, whereas there may also be a slight role for Abcg2. Furthermore, there was a reduced small intestine tissue exposure and SIC recovery of sotorasib in mice lacking Abcb1a/1b compared to wild-type mice, indicating a role of Abcb1a/1b in the intestinal disposition of sotorasib.

3.3. Brain penetration of sotorasib is boosted by the ABCB1/ABCG2 inhibitor elacridar

The brain exposure of sotorasib in wild-type mice was limited by mAbcb1a/1b and perhaps mAbcg2. If the same would apply to humans, this might affect the efficacy of sotorasib against brain (micro-) metastases. Therefore, we studied the effects of oral coadministration of elacridar, a dual ABCB1/ABCG2 inhibitor, on the brain distribution of sotorasib. Oral elacridar (50 mg/kg) or vehicle solution was administered to wild-type and *Abcb1a/1b;Abcg2*$^{-/-}$ mice 3 h prior to oral sotorasib administration to aim for complete inhibition of ABC transporters, based on the known T_{max} of elacridar around 4 h. This experiment was terminated 1 h after sotorasib administration.

The plasma exposure was slightly increased in *Abcb1a/1b;Abcg2*$^{-/-}$ compared to wild-type mice in the vehicle groups (Fig. 4, Suppl. Table 2, $P < 0.05$), but there were no significant shifts observed upon addition of elacridar between the vehicle and treatment groups. These plasma exposure results were quite similar to what we observed for these two mouse strains in the preceding experiments. In contrast,

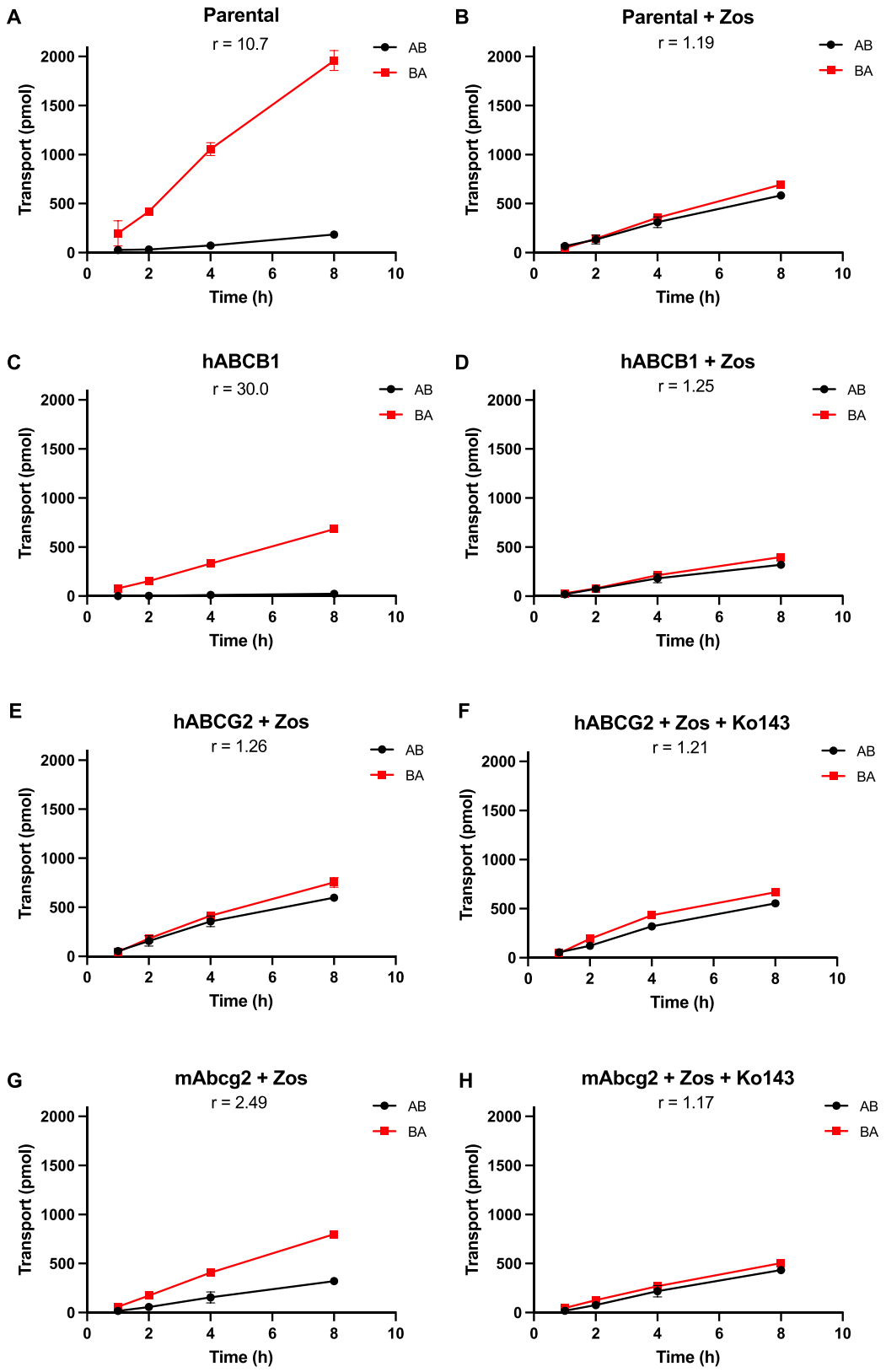

Fig. 1. Transepithelial transport of sotorasib (4 μM) studied in MDCK-II cells, either non-transduced (A, B), transduced with hABCB1 (C, D), hABCG2 (E, F) or mAbcg2 (G, H) cDNA. At t = 0 h, sotorasib was added only in the donor compartment, and the concentrations were measured in the acceptor compartment at t = 1, 2, 4, and 8 h. Data were plotted as cumulative sotorasib transport (pmol) per well over time (n = 3). B, D–H: Zosuquidar (Zos, 2 μM) was added to inhibit human and/or endogenous canine Abcb1. F and H: the ABCG2 inhibitor Ko143 (2 μM) was used to inhibit ABCG2/Abcg2. r, relative transport ratio. BA (■), translocation from the basolateral to the apical compartment; AB (●), translocation from the apical to the basolateral compartment. Data are presented as mean ± SD.

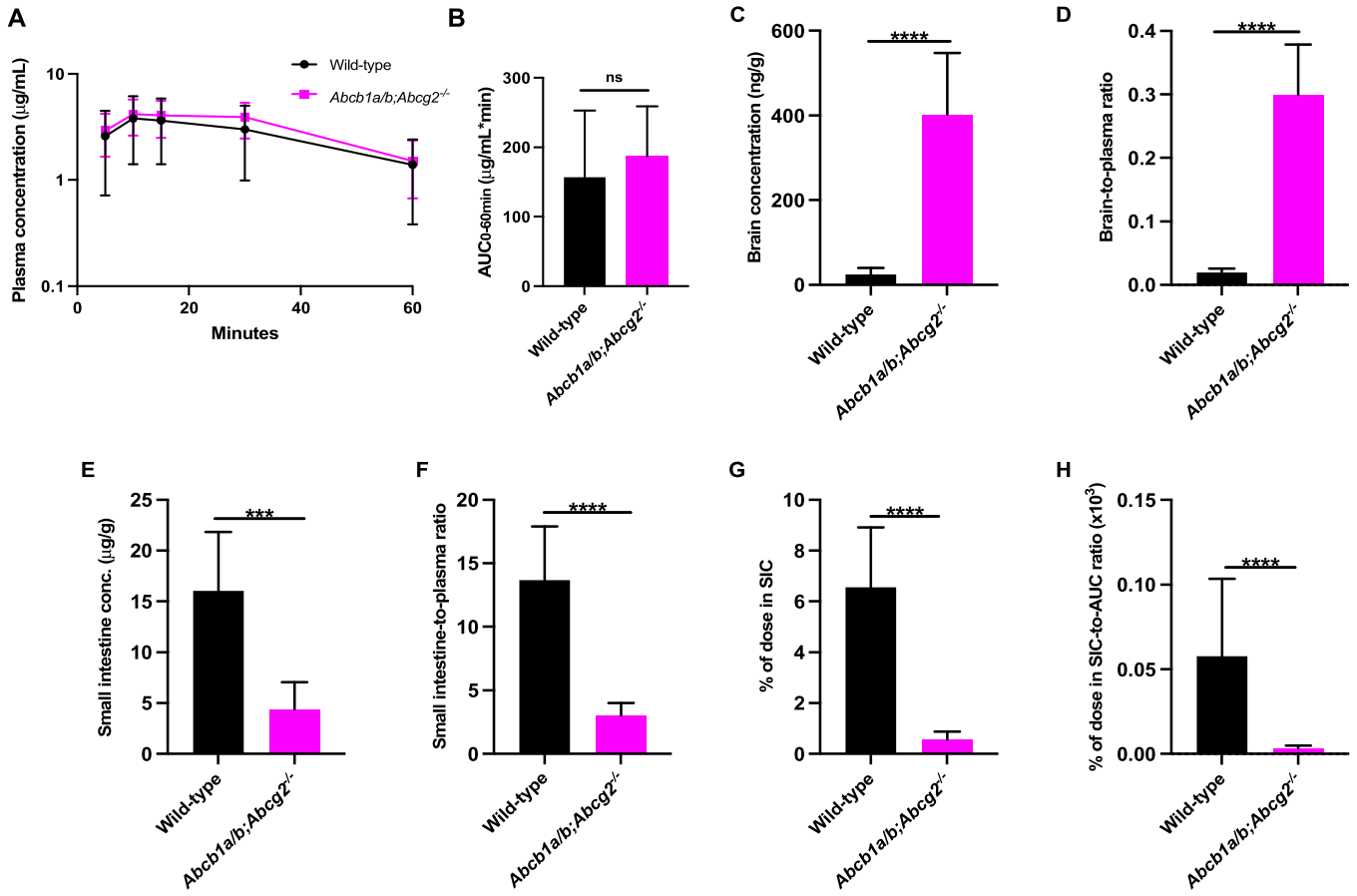

Fig. 2. Pharmacokinetic parameters in female wild-type and *Abcb1a/b;Abcg2*$^{-/-}$ mice over 1 h after oral administration of 20 mg/kg sotorasib (n = 6). A. Plasma concentration-time curve of sotorasib (semi-log scale). B. $AUC_{0-60min}$, area under the plasma concentration-time curve from 0 to the last time point (t = 60 min). C. Brain concentrations. D. Brain-to-plasma ratios. E. Small intestine tissue concentrations. F. Small intestine-to-plasma ratios. G. Percentage of recovered sotorasib dose in small intestinal content (SIC). H. Percentage of dose in SIC-to-AUC ratio. Data are presented as mean ± SD. ns, not significant; ***, $P < 0.001$; ****, $P < 0.0001$ compared to wild-type mice.

coadministration of elacridar instead of vehicle highly increased the brain concentration (12.7-fold, $P < 0.0001$) and brain-to-plasma ratio (7.5-fold, $P < 0.0001$) of sotorasib in wild-type mice. The levels obtained with elacridar in wild-type mice were similar to those in *Abcb1a/1b;Abcg2*$^{-/-}$ with or without elacridar, suggesting virtually complete inhibition of these transporters in the BBB (Fig. 4C and D, Suppl. Table 2). These brain parameters were not significantly different between *Abcb1a/1b;Abcg2*$^{-/-}$ mice with or without elacridar treatment. However, *Abcb1a/1b;Abcg2*$^{-/-}$ mice of both groups showed a 24-fold increase ($P < 0.0001$) in the brain concentration and an approximately 10-fold increase in the brain-to-plasma ratio compared to vehicle-pretreated wild-type, in part because of the somewhat higher plasma levels of sotorasib in *Abcb1a/1b;Abcg2*$^{-/-}$ mice. In this boosting experiment, no signs of acute CNS toxicity were observed.

The liver, spleen, and kidney dispositions of sotorasib were not noticeably affected by coadministration of elacridar in any of the strains (Suppl. Fig. 4A–F). In general, the tissue concentrations were slightly increased in *Abcb1a/1b;Abcg2*$^{-/-}$ with vehicle compared to wild-type mice pretreated with vehicle, reflecting the somewhat higher plasma concentration in *Abcb1a/1b;Abcg2*$^{-/-}$ mice. Interestingly, elacridar pretreatment in wild-type mice did lead to a significant reduction of the concentration (3.4-fold, $P < 0.001$) and percentage of dose of sotorasib in the small intestine including the contents (3.5-fold, $P < 0.001$) (Fig. 4E–H, Suppl. Table 2). In *Abcb1a/1b;Abcg2*$^{-/-}$ mice with elacridar pretreatment, there was a slight decrease in the concentration and recovered dose in small intestine and contents, even after correction for plasma AUC, although this was not statistically significant. These results suggest that mAbcb1a/b;Abcg2 activity in the intestine and liver was also almost completely inhibited by elacridar.

3.4. *In vivo impact of OATP1a/1b uptake transporters on liver disposition of sotorasib*

The impact of OATPs on the pharmacokinetics and tissue distribution of sotorasib was first evaluated in a 1-hour pilot experiment using female wild-type and *Oatp1a/1b*$^{-/-}$ mice after oral administration of 20 mg/kg sotorasib. The plasma $AUC_{0-60\ min}$ and C_{max} of *Oatp1a/1b*$^{-/-}$ mice were significantly increased (2.2-fold each) compared to wild-type (Suppl. Fig. 5A-B, Table 1, $P < 0.01$). Somewhat unexpectedly, the liver-to-plasma ratio of *Oatp1a/1b*$^{-/-}$ compared to wild-type mice was not significantly altered at the end of this experiment (Suppl. Fig. 5D). Oatp1a/1b transporters may also be expressed in the small intestine, possibly influencing the uptake or elimination of substrate drugs [21, 22]. The small intestine-to-plasma ratio was significantly reduced (2-fold) in *Oatp1a/1b*$^{-/-}$ compared to wild-type mice (Suppl. Fig. 5F, $P < 0.01$). Therefore, these results suggest that Oatp1a/1b transporters might have an influence on the oral availability and intestinal disposition of sotorasib, although the relative liver distribution was unchanged. We also observed a 1.6-fold increase (Suppl. Fig. 6B, $P < 0.01$) in the brain-to-plasma ratio of *Oatp1a/1b*$^{-/-}$ compared to wild-type mice, suggesting there is some role for Oatp1a/b in sotorasib brain disposition. The results further showed small, albeit significant, increases in the spleen-to-plasma ratio ($P < 0.01$) and lung-to-plasma ratio ($P < 0.05$) of *Oatp1a/1b*$^{-/-}$ mice, but not in the kidney-to-plasma ratio (Suppl.

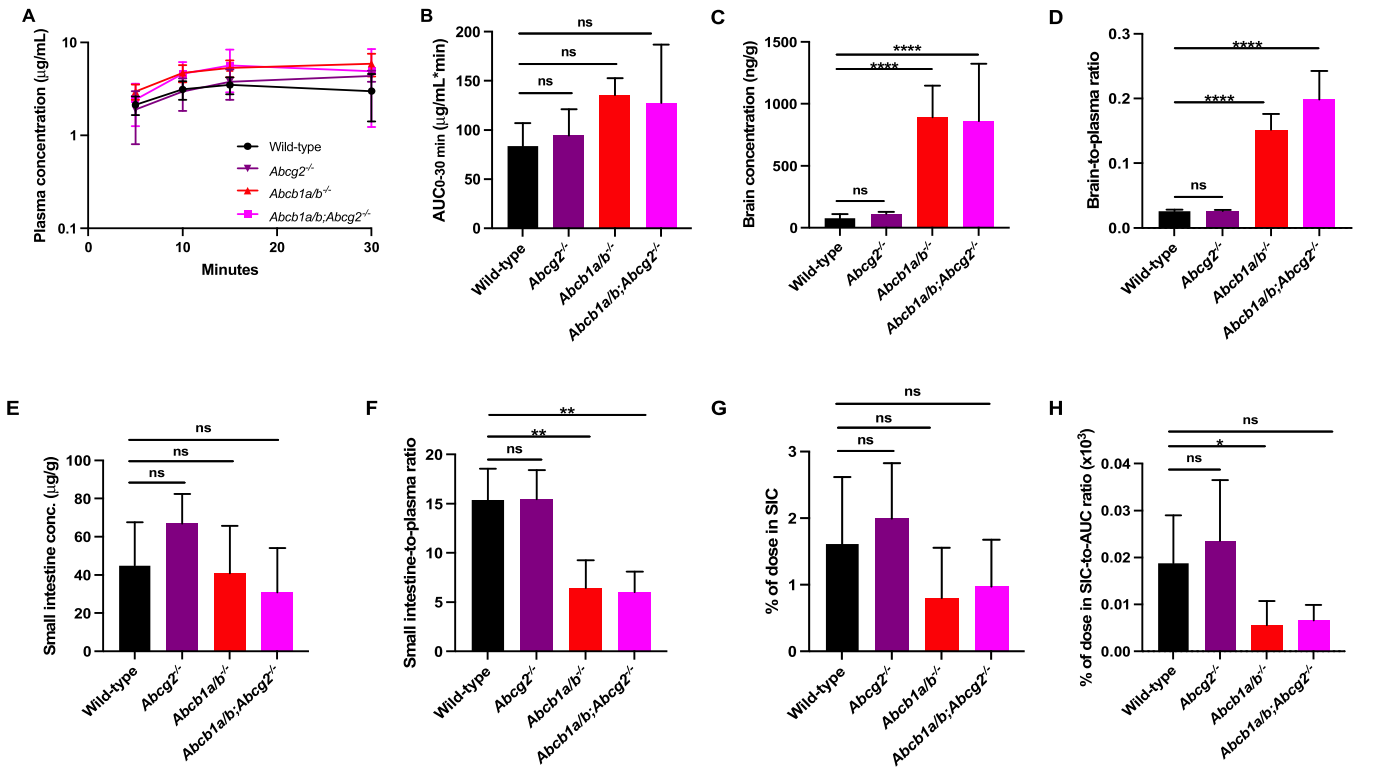

Fig. 3. Pharmacokinetic parameters in female wild-type, *Abcg2*$^{-/-}$, *Abcb1*$^{-/-}$, and *Abcb1a/b;Abcg2*$^{-/-}$ mice over 30 min after oral administration of 40 mg/kg sotorasib (n = 5–6). A. Plasma concentration-time curve of sotorasib (semi-log scale). B. $AUC_{0–30\ min}$, area under the plasma concentration-time curve from 0 to the last time point (t = 30 min). C. Brain concentrations. D. Brain-to-plasma ratios. E. Small intestine concentrations. F. Small intestine-to-plasma ratios. G. Percentage of recovered sotorasib dose in small intestinal content (SIC). H. Percentage of dose in SIC-to-AUC ratio. Data are presented as mean ± SD. ns, not significant compared to wild-type mice; **, $P < 0.01$; ****, $P < 0.0001$ compared to wild-type mice.

Fig. 6C-H and 7). These results suggest there is at best a limited influence of these uptake transporters on the general tissue distribution of sotorasib.

The plasma-concentration time curve of the pilot study (Suppl. Fig. 5A) suggested that primarily during the early absorption phase sotorasib developed differences between *Oatp1a/1b*$^{-/-}$ and wild-type mice. The early elimination of the drug seemed to occur similarly between the two strains. In view of the early T_{max} of sotorasib (~10 min) and in order to evaluate the early absorption phase of sotorasib, the termination time point in the follow-up study was 15 min. The sotorasib dose was also doubled to 40 mg/kg based on the pharmacokinetic parameters in humans [4]. In contrast to the pilot experiment, no statistically significant differences were found in plasma $AUC_{0–15\ min}$ and C_{max} between the two strains (Suppl. Fig. 8A-B, Table 1). However, the liver-to-plasma ratios of sotorasib in *Oatp1a/1b*$^{-/-}$ mice at 15 min were significantly decreased relative to wild-type values (2-fold, $P < 0.01$) (Suppl. Fig. 8D, Table 1). No meaningful or significant differences were found in the small intestine-to-plasma ratio (Suppl. Fig. 8F) or in the other analyzed tissues, possibly due to the early time point of termination (Suppl. Fig. 9 and 10). In summary, these data suggest that Oatp1a/1b transporters significantly contribute to the liver uptake of sotorasib early during the absorption phase, but they do not (yet) affect the plasma exposure.

3.5. Oral availability of sotorasib is limited by CYP3A

The potential influence of Cyp3a and CYP3A4 on the plasma pharmacokinetics and tissue distribution of oral sotorasib at a dose of 20 mg/kg was determined in a 4-hour study, using female wild-type, *Cyp3a*$^{-/-}$ and transgenic Cyp3aXAV mice (humanized mouse model; *Cyp3a*$^{-/-}$ with overexpression of human CYP3A4 in liver and small intestine). Sotorasib was rapidly absorbed with a T_{max} within 15–30 min in all mouse strains. The plasma exposure of sotorasib was significantly increased ($AUC_{0–4\ h}$ by 2.5-fold) in *Cyp3a*$^{-/-}$ compared to wild-type mice (Fig. 5A–C, Suppl. Table 3, $P < 0.01$). The C_{max} and $AUC_{0–4\ h}$ of sotorasib in Cyp3aXAV mice were significantly decreased by 1.8- ($P < 0.05$) and 3.9-fold ($P < 0.0001$), respectively, compared to *Cyp3a*$^{-/-}$ mice (Fig. 5C, Suppl. Table 3). These data indicate that CYP3A plays an important role in the metabolism of sotorasib, thereby limiting the plasma exposure. Further analysis of the semi-log plasma concentration-time curves (Fig. 5A) suggested that the main impact of mouse Cyp3a and especially human CYP3A4 occurred when plasma concentrations of sotorasib were relatively high (above 0.1 µg/mL). The elimination rate between the three strains became very similar below that concentration, suggesting that alternative clearance mechanisms than CYP3A biotransformation then started to dominate.

The impact of CYP3A on the tissue disposition of sotorasib at 4 h was also assessed. Unexpectedly, the brain-to-plasma ratio was reduced in *Cyp3a*$^{-/-}$ compared to wild-type mice (0.6-fold, $P < 0.01$), and increased in Cyp3aXAV compared to *Cyp3a*$^{-/-}$ as well as wild-type mice (4.3- and 1.7-fold, respectively, $P < 0.0001$) (Fig. 5E). However, the brain concentrations and brain-to-plasma ratios of sotorasib are likely strongly driven by the marked differences in plasma exposure between the three strains (Fig. 5A). This would especially have an impact if the release of sotorasib from the brain would be somewhat delayed relative to the (decreasing) plasma concentration because of some retention in the brain. In such cases, it is more appropriate to correct for the overall plasma exposure experienced by the brain (*i.e.*, plasma AUC). Indeed, when the brain accumulation was plotted for the three strains, we did not observe significant differences for sotorasib anymore (Fig. 5F).

Other analyzed tissues did not show any meaningful differences between the strains considering the tissue-to-plasma ratios, suggesting relatively rapid equilibration with plasma sotorasib (Suppl. Fig. 11 and 12). Moreover, the recovered percentage of dose in SIC from the

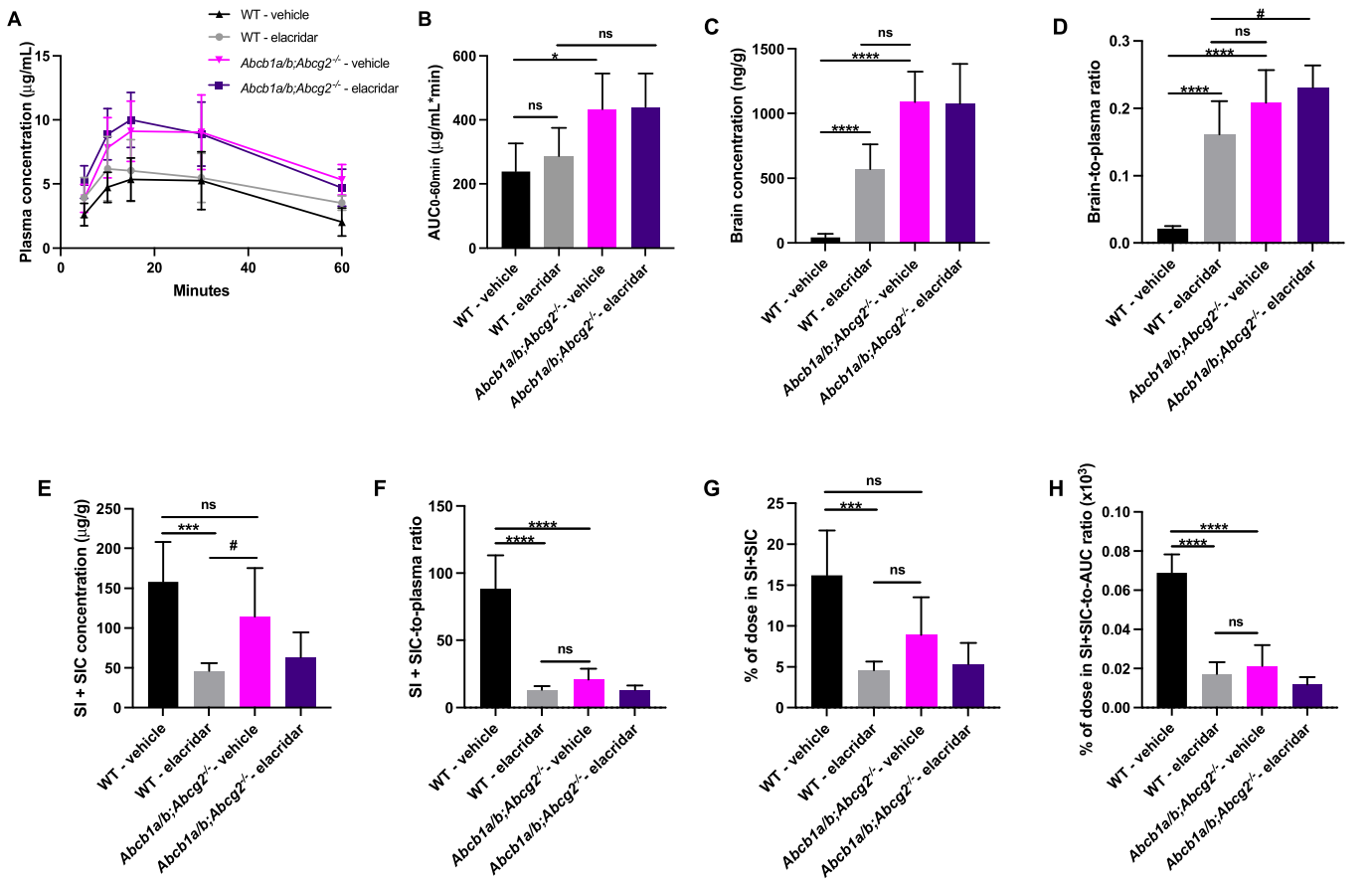

Fig. 4. Pharmacokinetic parameters of sotorasib in female wild-type and *Abcb1a/b;Abcg2*$^{-/-}$ mice over 1 h after oral administration of 40 mg/kg sotorasib and around 4 h after oral administration of 50 mg/kg elacridar or vehicle solution (n = 6). A. Plasma concentration-time curve of sotorasib. B. $AUC_{0–60\ min}$, area under the plasma concentration-time curve from 0 to the last time point (t = 60 min). C. Brain concentrations. D. Brain-to-plasma ratios (at 1 h after sotorasib administration). E. Small intestine + content (SI+SIC) concentrations. F. SI+SIC -to-plasma ratios (at 1 h after sotorasib administration). G. Percentage of recovered sotorasib dose in SI+SIC. H. Percentage of dose in SI+SIC-to-AUC ratio. Data are presented as mean ± SD. ns, not significant; *, $P < 0.05$; ***, $P < 0.001$; ****, $P < 0.0001$ compared to wild-type mice pretreated with vehicle solution. #, $P < 0.05$ compared to wild-type mice pretreated with elacridar.

administered sotorasib dose was significantly decreased in Cyp3aXAV compared to both other strains, reflecting the extensive sotorasib metabolism by transgenic human CYP3A4 (Suppl. Fig. 12, Suppl. Table 3, $P < 0.01$). Collectively, these results indicate that sotorasib is extensively metabolized by Cyp3a and CYP3A4, affecting both plasma and tissue exposure of sotorasib.

4. Discussion

As shown in our experiments, sotorasib was rapidly absorbed in all the examined mouse strains, which is in agreement with an earlier mouse study describing a T_{max} of 0.25 h for sotorasib [30]. This is also in line with the pharmacokinetic profile in humans with a median T_{max} of 2 h (range 0.3–6.0 h) and C_{max} of 7.50 µg/mL. The mean elimination (± SD) half-life in humans was approximately 5.5 ± 1.8 h after an administered dose of 960 mg daily [4]. Adjusting these values to smaller organisms, it is not unexpected that we observed relatively fast T_{max} and short elimination half-life in our mouse models for sotorasib, respectively 12.5 ± 3.9 and 39.7 ± 3.8 min

Our *in vitro* data show that hABCB1 could effectively transport sotorasib and mAbcg2 modestly, but hABCG2 not. However, it is known that the latter cell line has a relatively low expression of hABCG2, which needs to be taken into account when interpreting these results. With respect to hABCB1, our results are in line with a recent report by Madhyastha et al. in a similar MDCK-II-MDR1 (overexpression of ABCB1) transport assay documenting an efflux ratio of about 25 [30], similar to the ratio of 30 we found. The clear *in vitro* effect of ABCB1 on the transport of sotorasib is reflected in the impact that we observed on the brain and small intestine distribution in Abcb1a/1b-deficient mice.

The brain penetration of sotorasib was markedly increased in *Abcb1a/b*$^{-/-}$ and *Abcb1a/b;Abcg2*$^{-/-}$ mice compared to wild-type, but not noticeably in *Abcg2*$^{-/-}$ mice, which indicates that primarily ABCB1 can restrict brain exposure to sotorasib. In addition, there was no significant difference in brain penetration between *Abcb1a/b*$^{-/-}$ and *Abcb1a/b;Abcg2*$^{-/-}$ mice, together suggesting a minimal impact of ABCG2. The brain-to-plasma ratio of 0.02–0.03 in wild-type mice was fairly constant between the different time points and doses in our experiments (Table 1, Suppl. Table 1–3), and relatively low compared to many other targeted anticancer drugs. It is therefore unlikely that there is extensive retention of sotorasib in the brain. The brain penetration of sotorasib could be of clinical relevance, because the incidence of brain metastasis in $KRAS^{G12C}$-mutated NSCLC is approximately 50% [20]. Even though according to the FDA drug registration information drug exposure-response relationships are still unknown for sotorasib [31], it would be surprising if not a minimum drug concentration would be required for therapeutic efficacy of sotorasib in brain tumors. However, at what level that concentration might be, and whether it could be meaningfully improved by elacridar, could be an important aspect of future studies.

Coadministration of elacridar in mice to improve brain penetration of sotorasib showed virtually complete reversion of the influence of Abcb1a/1b transporters at the BBB. The ability to increase the brain penetration of sotorasib by inhibiting ABCB1 and ABCG2 using elacridar could be of clinical relevance, if we can achieve a similar level of

Table 1
Pharmacokinetic parameters of sotorasib 15 min and 1 h after oral administration of 40 or 20 mg/kg sotorasib, respectively, to female wild-type and Oatp1a/1b$^{-/-}$ mice.

Parameter	Genotype			
	15 min		1 h	
	Dose = 40 mg/kg		Dose = 20 mg/kg	
	Wild-type	*Oatp1a/b*$^{-/-}$	Wild-type	*Oatp1a/b*$^{-/-}$
$AUC_{0–15\ min}$, μg. min/mL	61.66 ± 19.08	78.00 ± 41.75	ND	ND
Fold increase $AUC_{0–15\ min}$	1.00	1.27	ND	ND
$AUC_{0–60\ min}$, μg. min/mL	ND	ND	156.87 ± 96.38	343.34 ± 74.07**
Fold increase $AUC_{0–60\ min}$	ND	ND	1.00	2.19
C_{max}, μg/mL	6.63 ± 1.52	7.90 ± 3.67	4.00 ± 2.34	8.66 ± 1.57**
T_{max}, min	14.2 ± 2.0	12.0 ± 2.7	17.5 ± 9.9	11.7 ± 4.1
C_{brain}, ng/g	156.5 ± 40.99	209.7 ± 112.4	24.75 ± 14.85	84.39 ± 22.43***
Fold increase C_{brain}	1.00	1.32	1.00	3.41
Brain-to-plasma ratio	0.024 ± 0.003	0.027 ± 0.005	0.020 ± 0.006	0.032 ± 0.004**
Fold increase ratio	1.00	1.10	1.00	1.63
C_{Liver}, μg/g	31.55 ± 10.0	18.03 ± 8.397	2.352 ± 1.544	4.249 ± 1.916
Fold change C_{Liver}	1.00	0.57	1.00	1.81
Liver-to-plasma ratio	4.99 ± 1.57	2.46 ± 0.61**	1.70 ± 0.36	1.56 ± 0.51
Fold change ratio	1.00	0.49	1.00	0.92
SIC (% of dose)	1.17 ± 0.64	0.92 ± 0.77	6.56 ± 2.35	10.82 ± 4.06
Fold change	1.00	0.79	1.00	1.65

Data are presented as mean ± S.D. (n = 5–6). $AUC_{0–t}$, area under the plasma concentration-time curve from 0 to the last time point (t = 15 or 60 min); C_{max}, maximum concentration in plasma; T_{max}, time point (min) of maximum plasma concentration; SIC, small intestinal content; SIC (% of dose), sotorasib in SIC as percentage of dose. *, $P < 0.05$; **, $P < 0.01$; ***, $P < 0.001$ compared to wild-type mice. ND = not determined.

inhibition in the human BBB. Interestingly, we did not observe any sign of acute CNS toxicity of sotorasib in either Abcb1a/1b-, and/or Abcg2-deficient mouse strains or elacridar-treated mice, in contrast to, for example, brigatinib, which showed lethal toxicity in *Abcb1a/1b;Abcg2*$^{-/-}$ mice [32]. While elacridar inhibits both ABCB1 and ABCG2, early studies in humans indicated it is quite well tolerated [33]. Currently a main limiting factor for application of elacridar in humans is its low oral availability, but this issue is currently addressed in our institute by optimizing formulations. Although this approach in humans is still in its infancy, it is worth noting that elacridar as a relatively safe combined inhibitor of ABCB1 and ABCG2 might be relevant for a large number of anticancer (and other) drugs that are kept out of the brain by ABCB1 and/or ABCG2 in the BBB.

The significantly lower percentage of the sotorasib dose recovered in SIC of Abcb1a/1b-deficient mice further indicated a significant influence of Abcb1a/1b efflux transporters on the small intestine disposition of sotorasib, which could be completely reversed by elacridar. Possible explanations for these effects could be: ABCB1 in the small intestine transports sotorasib directly back into the intestinal lumen, resulting in higher concentrations in the small intestinal content; or ABCB1 in the hepatocytes mediates the hepatobiliary excretion of sotorasib, or a combination of both of processes.

While we show here that a highly effective ABCB1 inhibitor such as elacridar can affect the pharmacokinetics of sotorasib, it is conversely also possible that sotorasib, which has been described as an ABCB1 inhibitor in the FDA registration information [9,31], albeit at high concentrations, may also alter the pharmacokinetics of coadministered anticancer drugs that are strongly affected by ABCB1 function. Due caution should therefore be used when combining sotorasib with other drugs that may be strongly affected by ABCB1 activity.

Our data suggest that tumors (over)expressing ABCB1 would likely show intrinsic or acquired resistance to sotorasib. We expect that at least some $KRAS^{G12C}$ tumors during sotorasib treatment could readily express more ABCB1 on their surfaces and thus acquire resistance to sotorasib, alongside other types of acquired resistance to $KRAS^{G12C}$ inhibitors described in literature [34–37]. In lung tumor cells, there is normally only a low ABCB1 expression level. However, this can alter after chemotherapy exposure and can result in acquired drug resistance [38,39]. Vesel et al. showed that in primary cancer tissues of adeno- and squamous cell carcinomas, the two most common NSCLC subtypes, ABCB1 and ABCG2 expression levels could change [40]. Treatment of NSCLC patients with cisplatin could lead to upregulation of both ABCB1 and ABCG2 expression and hence their activity [40]. Given the role of ABCB1 in extruding sotorasib from cells, it is therefore imaginable that such overexpression will lead to relative resistance of these NSCLC tumors to sotorasib. Due to these different resistance mechanisms, combinational therapy (including EGFR and MEK inhibitors, as well as PD-1/PD-L1 inhibitors) could perhaps improve the efficacy of sotorasib, which is currently being investigated in clinical trials [41].

Furthermore, we studied mouse Oatp1a/1b uptake transporters, which may play a modest role in liver distribution of sotorasib and its oral availability. While it is currently unknown whether sotorasib enters most cells primarily by passive diffusion or mediated transport, our data suggest that, under the right circumstances, mouse Oatp1a/1b proteins can at least partially contribute to the hepatocellular uptake of sotorasib. In the pilot experiment the observed differences in plasma exposure occurred especially during the absorption phase, whereas in the follow-up only slight increases in $AUC_{0–15\ min}$ and C_{max} were observed, albeit not statistically significant. This could be due to higher inter-individual variation between mice at this early time point of termination, and possibly due to the doubling in dose leading to saturation of Oatp1a/1b transporters.

Apart from plasma exposure, liver uptake is one of the most important parameters to study functional effects of Oatp1a/1b. Somewhat unexpectedly, we only observed a slight decrease in the liver-to-plasma ratio in the pilot, but we did observe a significant reduction of the liver disposition in *Oatp1a/1b*$^{-/-}$ mice in the 15-min follow-up study, suggesting a role of mOatp1a/1b in liver exposure to sotorasib early after administration. In *Oatp1a/1b*$^{-/-}$ mice, the increase in plasma exposure might be due to downregulation of one or more protein(s), which limit plasma exposure. The increased plasma levels may compensate the reduced liver-to-plasma ratio in Oatp1a/1b-deficient mice, which could explain why we did not observe lower liver-to-plasma ratios in *Oatp1a/1b*$^{-/-}$ mice during the pilot. In the main experiment, this unspecified protein could be somewhat saturated, therefore the effects of Oatp1a/1b became more important and could mediate in liver uptake of sotorasib. Whether the small decreases we observed in spleen- and lung-to-plasma ratios of sotorasib in *Oatp1a/1b*$^{-/-}$ mice are indicative of a minor functional contribution of Oatp1a/1b to the tissue uptake of sotorasib in these organs is uncertain. Broader studies, including more optimal substrates for the Oatp1a/1b transporters may be necessary to reliably establish such a function in these organs. Given the modest effects of Oatp1a/1b transporters on liver and plasma disposition of sotorasib, and the high inter-individual variation shortly after drug administration, it is not surprising that the intestinal content disposition did not demonstrate clear shifts. Based on these results, we cannot exclude that OATP1a/b transporters might have a noticeable impact on sotorasib systemic exposure. However, the FDA registration information mentions that a single administration of rifampin, an OATP1B1/1B3 inhibitor, in humans did not clinically meaningfully affect the exposure to sotorasib, suggesting that there is probably limited risk in this respect [9,31].

The plasma exposure of sotorasib was significantly higher in Cyp3a-deficient mice and lower in transgenic Cyp3aXAV mice. This suggests that CYP3A plays a prominent role in the oral availability and

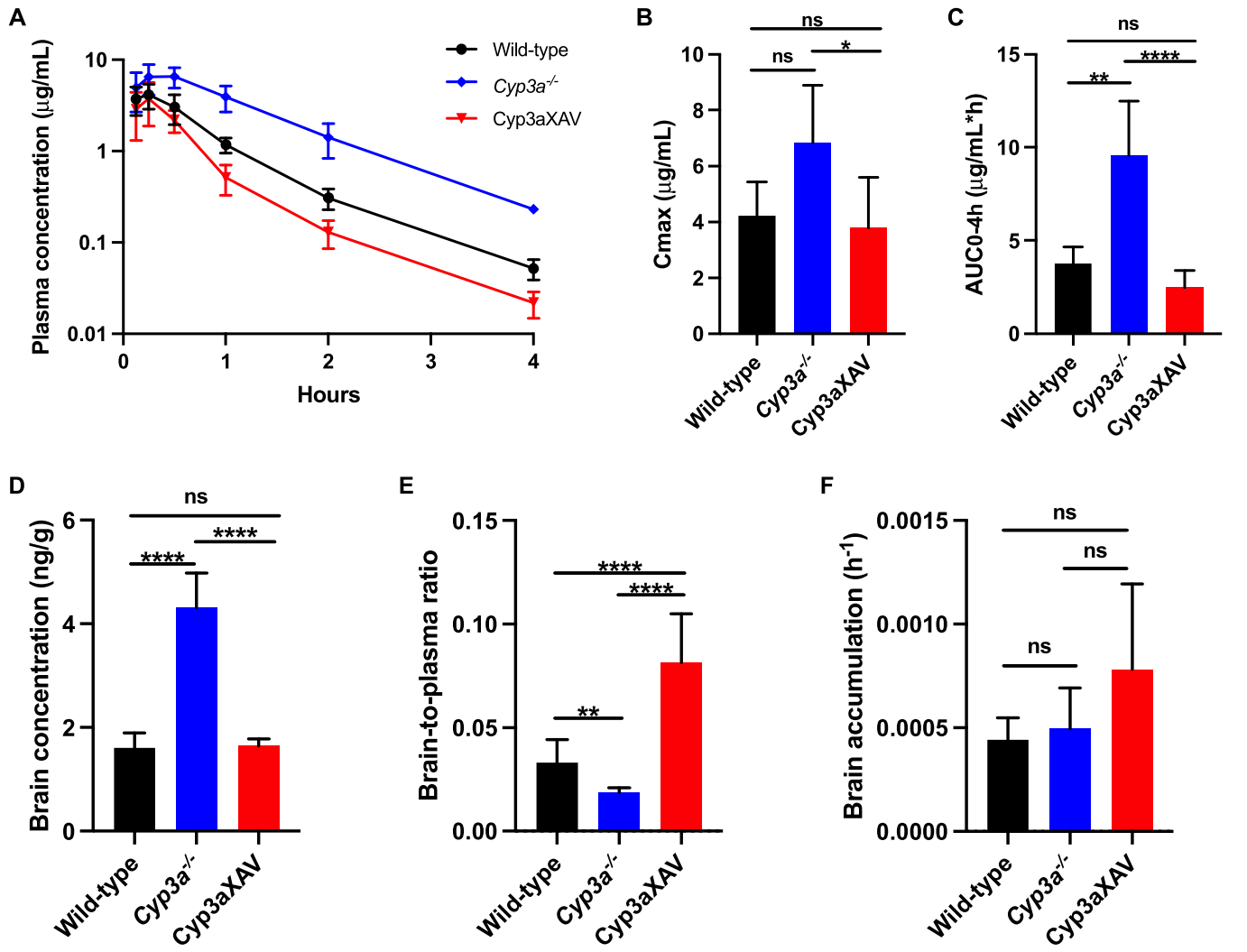

Fig. 5. Pharmacokinetic parameters of sotorasib in female wild-type, *Cyp3a*$^{-/-}$, and Cyp3aXAV (transgenic overexpression of human CYP3A4 in liver and intestine) mice over 4 h after oral administration of 20 mg/kg sotorasib (n = 6). A. Plasma concentration-time curve (semi-log scale) of sotorasib. B. C_{max}, maximum concentration in plasma. C. $AUC_{0-4\ h}$, area under the plasma concentration-time curve from 0 to the last time point (t = 4 h). D. Brain concentrations. E. Brain-to-plasma ratios. F. Brain accumulation per hour. Data are presented as mean ± SD. ns, not significant; *, $P < 0.05$; **, $P < 0.01$; ****, $P < 0.0001$ compared to wild-type or *Cyp3a*$^{-/-}$ mice.

metabolism of sotorasib in mice. The overall plasma and, consequently, tissue exposure to sotorasib was reduced in Cyp3aXAV compared to *Cyp3a*$^{-/-}$, as well as wild-type mice. This could be due to a higher amount of CYP3A4 in the intestine or to higher efficiency of human CYP3A4 compared to murine Cyp3a in metabolizing sotorasib. These results are in agreement with the FDA rapport indicating that sotorasib is primarily metabolized by CYP3A4 [9]. Interestingly, the elimination rate between the three different strains seems to be fairly similar at later time points and below a sotorasib plasma concentration of approximately 0.1 µg/mL. This suggests that there are alternative clearance mechanisms that take over the elimination process of sotorasib at lower systemic concentrations. However, as M24, the primary known metabolite formed from sotorasib through CYP3A, is known to have no activity against ERK1/2, it is likely that CYP3A activity will decrease the therapeutic pharmacodynamic effects of sotorasib [31,42]. Based on these mouse model results, coadministration of (strong) CYP3A4 inhibitors or inducers might alter the systemic exposure to sotorasib, and such coadministration should be only considered with caution. However, the FDA registration information mentions that the CYP3A (and ABCB1) inhibitor itraconazole did not have clinically relevant effects on sotorasib exposure, but that repeated administration of the CYP3A4-inducing compound rifampin decreases sotorasib exposure (AUC) by about 2-fold [31]. This suggests that in patients CYP3A4 induction presents more of a DDI risk for sotorasib than CYP3A4 inhibition.

5. Conclusion

Sotorasib is a potent *in vivo* substrate for the efflux transporter ABCB1 and the metabolizing enzyme CYP3A4, whereas it probably is a moderate substrate for Oatp1a/1b uptake transporters. The brain penetration of sotorasib is highly restricted by ABCB1, alone or in combination with ABCG2. Coadministration of the booster elacridar can strongly enhance the brain disposition of orally administered sotorasib without obvious acute CNS toxicity or marked changes in systemic exposure in mice. Our results suggest that OATP or CYP3A4 polymorphisms or coadministration of OATP and/or CYP3A4 inducers and, perhaps, inhibitors could potentially affect the systemic exposure of sotorasib. The obtained results could be useful for further optimization of the safety and efficacy of sotorasib in clinical use.

Funding sources

This research did not receive any specific grant from funding agencies in the public, commercial, or not-for-profit sectors.

CRediT authorship contribution statement

Nancy H.C. Loos: Conceptualization, Formal analysis, Investigation, Methodology, Visualization, Writing – original draft. **Irene A. Retmana:** Sample bioanalysis, Visualization, Writing – review & editing. **Wenlong Li:** Contribution in performing transwell experiment and mouse experiments pilot study, Writing – review & editing. **Margarida L.F. Martins:** Contribution in performing mouse experiments follow-up study, Writing – review & editing. **Maria C. Lebre:** Contributed the reagents, materials, and mice, Writing – review & editing. **Rolf W. Sparidans:** Supervision of bioanalytical analysis, Writing – review & editing. **Jos H. Beijnen:** Supervision, Writing – review content. **Alfred H. Schinkel:** Conceptualization, Supervision, Formal analysis, Writing – review & editing. All authors commented on and approved the manuscript.

Declaration of Competing Interest

The research group of A.H. Schinkel receives revenue from commercial distribution of some of the mouse strains used in this study. The other authors declare that they have no competing financial or other interests that could have influenced the published work in this paper.

Data Availability

The data that supports the findings of this study are available in the supplementary material of this article.

Acknowledgements

We would like to thank Yaogeng Wang for his assistance in executing some of the mouse experiments.

Appendix A. Supporting information

Supplementary data associated with this article can be found in the online version at doi:10.1016/j.phrs.2022.106137.

References

[1] A.D. Cox, et al., Drugging the undruggable RAS: mission possible? Nat. Rev. Drug Discov. 13 (11) (2014) 828–851.
[2] I.A. Prior, P.D. Lewis, C. Mattos, A comprehensive survey of Ras mutations in cancer, Cancer Res. 72 (10) (2012) 2457–2467.
[3] A. Biernacka, et al., The potential utility of re-mining results of somatic mutation testing: KRAS status in lung adenocarcinoma, Cancer Genet. 209 (5) (2016) 195–198.
[4] D.S. Hong, et al., KRAS(G12C) inhibition with sotorasib in advanced solid tumors, New Engl. J. Med. 383 (13) (2020) 1207–1217.
[5] J. Neumann, et al., Frequency and type of KRAS mutations in routine diagnostic analysis of metastatic colorectal cancer, Pathol. Res. Pract. 205 (12) (2009) 858–862.
[6] S. Ouerhani, A.B. Elgaaied, The mutational spectrum of HRAS, KRAS, NRAS and FGFR3 genes in bladder cancer, Cancer Biomark. 10 (6) (2011) 259–266.
[7] B.A. Lanman, et al., Discovery of a covalent inhibitor of KRAS(G12C) (AMG 510) for the treatment of solid tumors, J. Med. Chem. 63 (1) (2020) 52–65.
[8] J. Canon, et al., The clinical KRAS(G12C) inhibitor AMG 510 drives anti-tumour immunity, Nature 575 (7781) (2019) 217–223.
[9] FDA, U.S.F.a.D.A., Prescribing information LUMAKRAS™ (sotorasib) tablets, for oral use, 2021.
[10] F. Oesch, Importance of knowledge on drug metabolism for the safe use of drugs in humans, Drug Metab. Rev. 41 (3) (2009) 298–300.
[11] K.M. Giacomini, et al., Membrane transporters in drug development, Nat. Rev. Drug Discov. 9 (3) (2010) 215–236.
[12] A.H. Schinkel, J.W. Jonker, Mammalian drug efflux transporters of the ATP binding cassette (ABC) family: an overview, Adv. Drug Deliv. Rev. 55 (1) (2003) 3–29.
[13] S. Choudhuri, C.D. Klaassen, Structure, function, expression, genomic organization, and single nucleotide polymorphisms of human ABCB1 (MDR1), ABCC (MRP), and ABCG2 (BCRP) efflux transporters, Int. J. Toxicol. 25 (4) (2006) 231–259.
[14] G. Szakács, et al., The role of ABC transporters in drug absorption, distribution, metabolism, excretion and toxicity (ADME-Tox), Drug Discov. Today 13 (9–10) (2008) 379–393.
[15] D.S. Miller, ABC transporter regulation by signaling at the blood-brain barrier: relevance to pharmacology, Adv. Pharmacol. 71 (2014) 1–24.
[16] S.C. Tang, et al., Impact of P-glycoprotein (ABCB1) and breast cancer resistance protein (ABCG2) gene dosage on plasma pharmacokinetics and brain accumulation of dasatinib, sorafenib, and sunitinib, J. Pharmacol. Exp. Ther. 346 (3) (2013) 486–494.
[17] X. Bao, et al., Protein expression and functional relevance of efflux and uptake drug transporters at the blood-brain barrier of human brain and glioblastoma, Clin. Pharmacol. Ther. 107 (5) (2020) 1116–1127.
[18] A.H. Schinkel, et al., P-glycoprotein in the blood-brain barrier of mice influences the brain penetration and pharmacological activity of many drugs, J. Clin. Investig. 97 (11) (1996) 2517–2524.
[19] J. Goncalves, et al., Relevance of breast cancer resistance protein to brain distribution and central acting drugs: a pharmacokinetic perspective, Curr. Drug Metab. 19 (12) (2018) 1021–1041.
[20] P. Tomasini, et al., EGFR and KRAS mutations predict the incidence and outcome of brain metastases in non-small cell lung cancer, Int. J. Mol. Sci. 17 (2016) 12.
[21] A. Kalliokoski, M. Niemi, Impact of OATP transporters on pharmacokinetics, Br. J. Pharmacol. 158 (3) (2009) 693–705.
[22] N. Couto, et al., Quantitative proteomics of clinically relevant drug-metabolizing enzymes and drug transporters and their intercorrelations in the human small intestine, Drug Metab. Dispos. 48 (4) (2020) 245–254.
[23] O. Lolodi, et al., Differential regulation of CYP3A4 and CYP3A5 and its implication in drug discovery, Curr. Drug Metab. 18 (12) (2017) 1095–1105.
[24] U.M. Zanger, M. Schwab, Cytochrome P450 enzymes in drug metabolism: regulation of gene expression, enzyme activities, and impact of genetic variation, Pharmacol. Ther. 138 (1) (2013) 103–141.
[25] J.K. Lamba, et al., Genetic contribution to variable human CYP3A-mediated metabolism, Adv. Drug Deliv. Rev. 54 (10) (2002) 1271–1294.
[26] I.A. Retmana, et al., Quantification of KRAS inhibitor sotorasib in mouse plasma and tissue homogenates using liquid chromatography-tandem mass spectrometry, J. Chromatogr. B Anal. Technol. Biomed. Life Sci. 1174 (2021), 122718.
[27] R. Evers, et al., Drug export activity of the human canalicular multispecific organic anion transporter in polarized kidney MDCK cells expressing cMOAT (MRP2) cDNA, J. Clin. Investig. 101 (7) (1998) 1310–1319.
[28] B. Poller, et al., Double-transduced MDCKII cells to study human P-glycoprotein (ABCB1) and breast cancer resistance protein (ABCG2) interplay in drug transport across the blood-brain barrier, Mol. Pharm. 8 (2) (2011) 571–582.
[29] J.W. Jonker, et al., Role of breast cancer resistance protein in the bioavailability and fetal penetration of topotecan, J. Natl. Cancer Inst. 92 (20) (2000) 1651–1656.
[30] N. Madhyastha, et al., Validated HPLC-MS/MS method for quantitation of AMG 510, a KRAS G12C inhibitor, in mouse plasma and its application to a pharmacokinetic study in mice, Biomed. Chromatogr. 35 (4) (2021), e5043.
[31] (FDA) U.S.F.a.D.A., NDA/BLA Multi-disciplinary Review and Evaluation {NDA 214665} LUMAKRAS™ (sotorasib), 2020.
[32] W. Li, et al., P-glycoprotein and breast cancer resistance protein restrict brigatinib brain accumulation and toxicity, and, alongside CYP3A, limit its oral availability, Pharm. Res. 137 (2018) 47–55.
[33] R.P. Dash, R. Jayachandra Babu, N.R. Srinivas, Therapeutic potential and utility of elacridar with respect to P-glycoprotein inhibition: an insight from the published in vitro, preclinical and clinical studies, Eur. J. Drug Metab. Pharm. 42 (6) (2017) 915–933.
[34] V. Dunnett-Kane, et al., Mechanisms of resistance to KRAS(G12C) inhibitors, Cancers 13 (2021) 1.
[35] A. Singh, et al., A gene expression signature associated with "K-Ras addiction" reveals regulators of EMT and tumor cell survival, Cancer Cell 15 (6) (2009) 489–500.
[36] J.Y. Xue, et al., Rapid non-uniform adaptation to conformation-specific KRAS (G12C) inhibition, Nature 577 (7790) (2020) 421–425.
[37] M.B. Ryan, et al., Vertical pathway inhibition overcomes adaptive feedback resistance to KRAS(G12C) inhibition, Clin. Cancer Res. 26 (7) (2020) 1633–1643.
[38] I. Zawadzka, et al., The impact of ABCB1 gene polymorphism and its expression on non-small-cell lung cancer development, progression and therapy - preliminary report, Sci. Rep. 10 (1) (2020) 6188.
[39] D. Campa, et al., A comprehensive study of polymorphisms in ABCB1, ABCC2 and ABCG2 and lung cancer chemotherapy response and prognosis, Int. J. Cancer 131 (12) (2012) 2920–2928.
[40] M. Vesel, et al., ABCB1 and ABCG2 drug transporters are differentially expressed in non-small cell lung cancers (NSCLC) and expression is modified by cisplatin treatment via altered Wnt signaling, Respir. Res. 18 (1) (2017) 52.
[41] C.R. Lindsay, et al., On target: rational approaches to KRAS inhibition for treatment of non-small cell lung carcinoma, Lung Cancer 160 (2021) 152–165.
[42] J.A. Werner, et al., Mercapturate pathway metabolites of sotorasib, a covalent inhibitor of KRAS(G12C), are associated with renal toxicity in the Sprague Dawley rat, Toxicol. Appl. Pharmacol. 423 (2021), 115578.